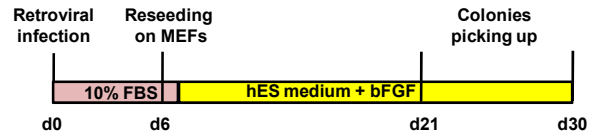
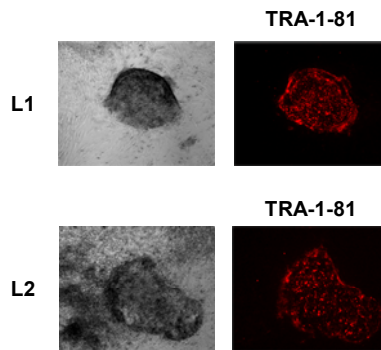


a

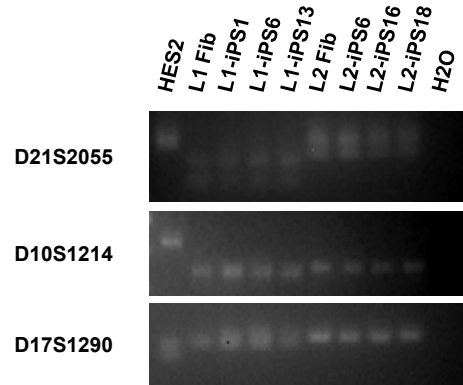


b

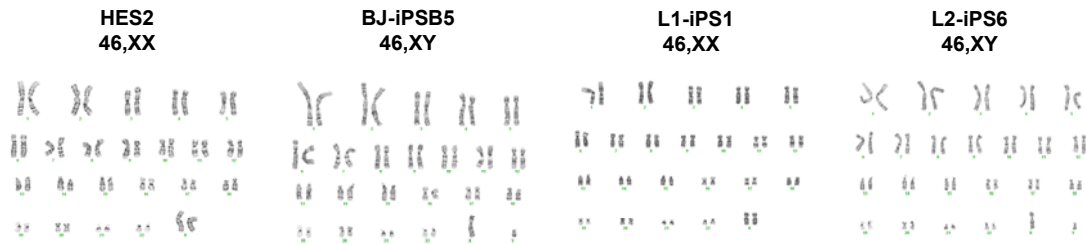


Supplementary Figure 1. LS-iPSC formation. **a**, Schematic representation of iPSC generation. **b**, Typical image of a TRA-1-81 positive colony growing in the plate three weeks after infection.

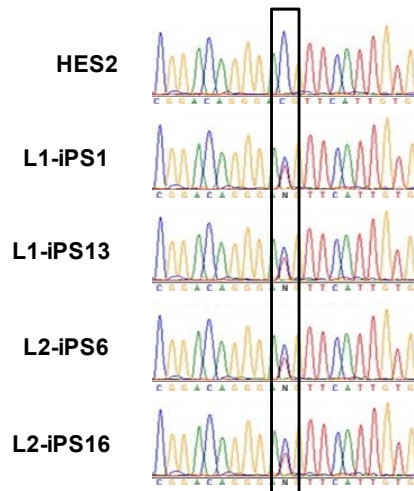
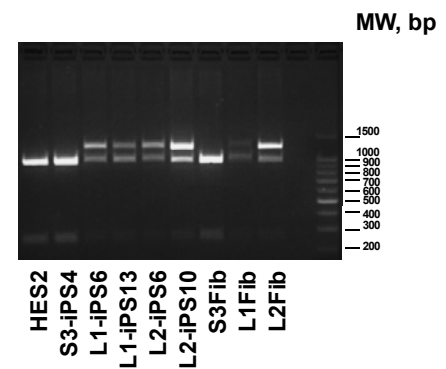
a



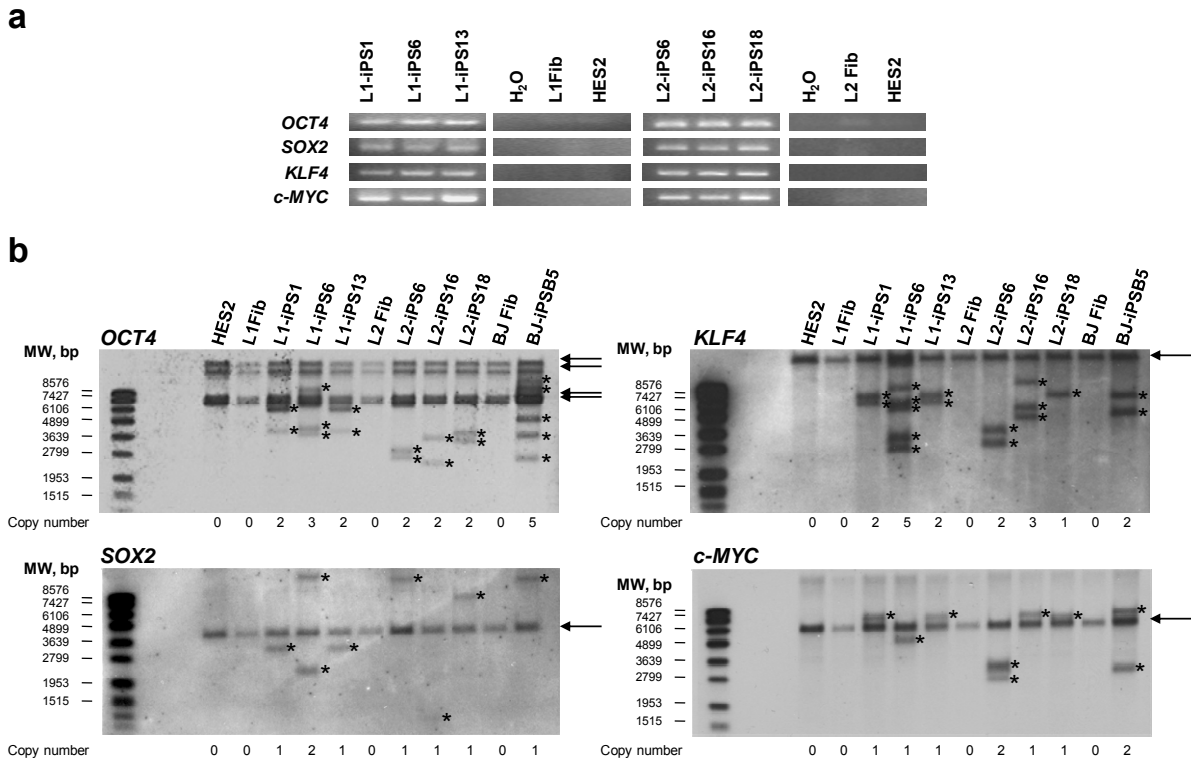
b



Supplementary Figure 2. LS-iPSC lines are derived from their parental fibroblasts and maintain normal karyotypes. **a**, We PCR amplified across three discrete genomic loci containing highly variable numbers of tandem repeats with different primer sets (D10S1214, D17S1290, and D21S2055). The resulting amplification patterns confirmed that each iPSC line is derived from its indicated parental fibroblast. **b**, G-banding of HES2 cell line, wild-type iPS clone BJ-iPSB5, and LS-iPSC lines (one clone of each patient) demonstrates normal diploid chromosomal contents.

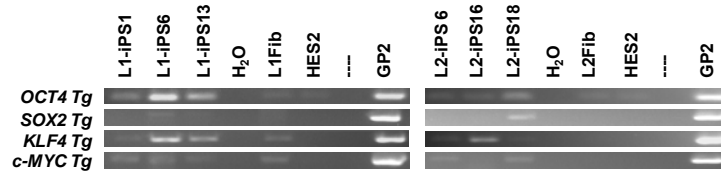
a**b**

Supplementary Figure 3. *PTPN11* T468M mutation analysis in LS-iPSC and fibroblasts. **a**, The T468M point mutation in exon 12 of one allele of *PTPN11* gene was verified by DNA sequencing. **b**, We amplified by RT-PCR a 1.2 Kb region containing the mutation sequence and the DNA was digested with BsmFI, an enzyme which cuts the 5'-GGGAC(N)₁₀-3' sequence contained in wt allele but not in the mutant. In all the LS samples an undigested 1.2 Kb band was observed.

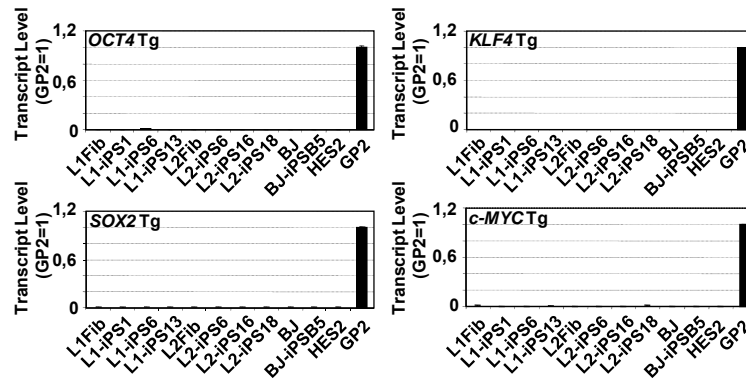


Supplementary Figure 4. Retroviral transgenes integration in iPSC. **a**, Transgene-specific primers were used to amplify *OCT4*, *SOX2*, *KLF4* and *c-MYC*. Three LS-derived iPSC lines from each patient were analyzed, and HES2 cells and parental fibroblasts were used as negative controls. **b**, Southern blot analyses of Bgl-II digested gDNA extracted from HES2 cells, parental fibroblasts and iPSC, using DIG-labeled DNA probes against *OCT4*, *SOX2*, *KLF4* and *c-MYC*. Retrovirally-inserted transgenic copies of these genes are indicated by asterisks and the number of detected bands is shown at the bottom. The parental fibroblasts and HES2 cells share bands in common with all the iPSC lines (arrowheads), which reflect the endogenous loci (including potential pseudogenes).

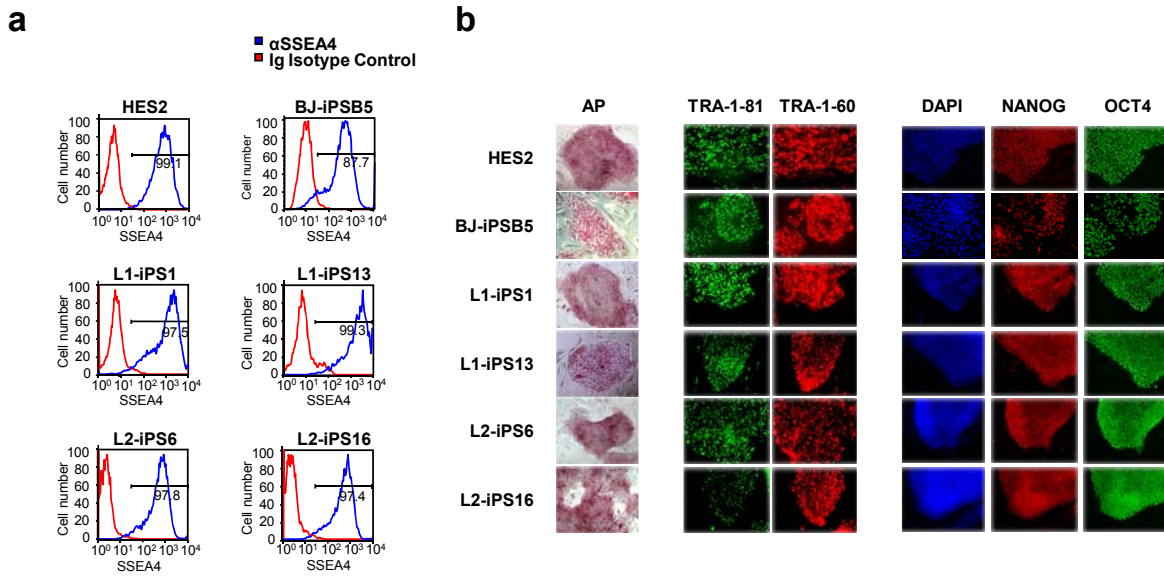
a



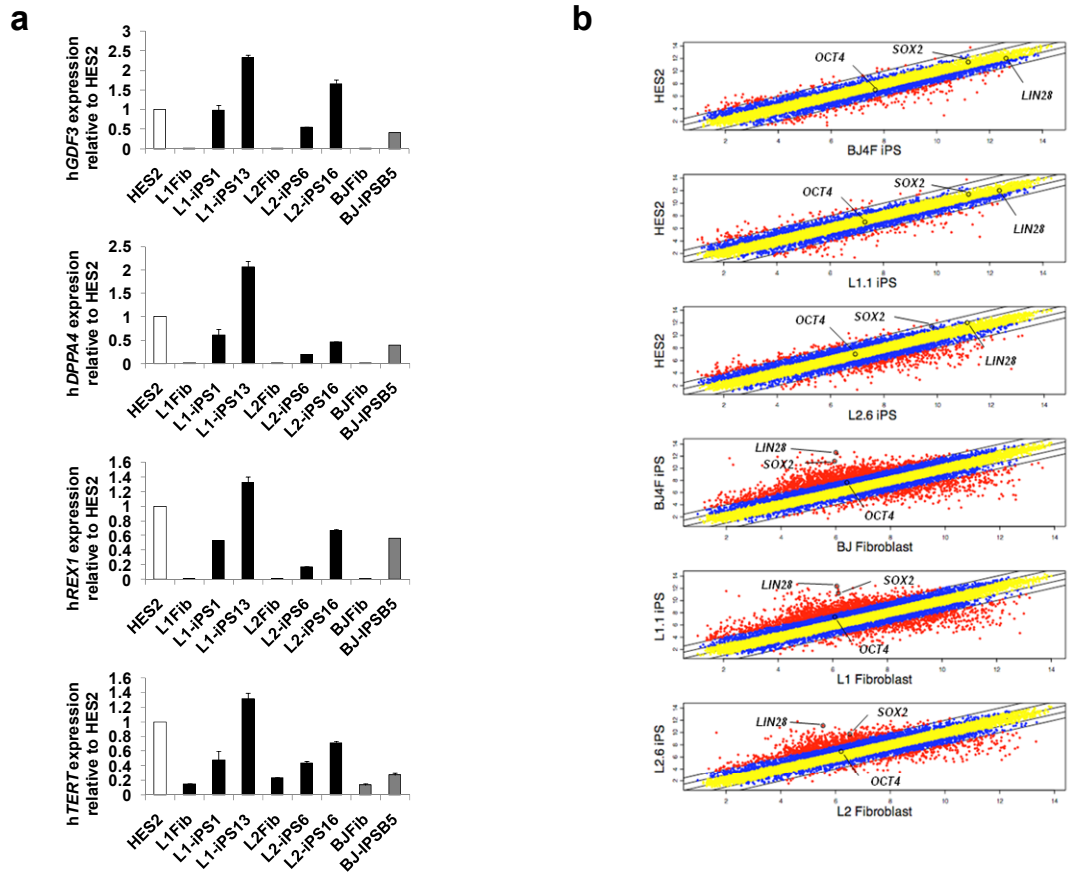
b



Supplementary Figure 5. Retroviral transgenes silencing in iPSC lines. a, Transgene-specific primers were used to determine *OCT4*, *SOX2*, *KLF4* and *c-MYC* expression. **b,** qPCR analysis of retroviral transgene (Tg) expression. Results were normalized against β -*ACTIN* and plotted relative to the expression levels in transfected GP2 cells.

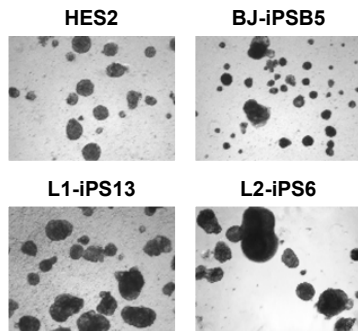


Supplementary Figure 6. LS-iPSC expressed markers common to pluripotent cells. **a**, SSEA4 expression was determined by flow cytometry in two iPSC lines derived from two LEOPARD syndrome (LS) patients (L1-iPS1, L1-iPS13, L2-iPS6 and L2-iPS16), and a wt-iPSC line derived from BJ fibroblasts (BJ-iPSB5). HES2 cell line was used as positive control. **b**, HES2 and iPSC were grown on MEFs, and the day of the immunocytochemistry cells were fixed and stained for the pluripotency markers, alkaline phosphatase (AP), TRA-1-81, TRA-1-60, NANOG and OCT4. Nuclei were stained with DAPI.

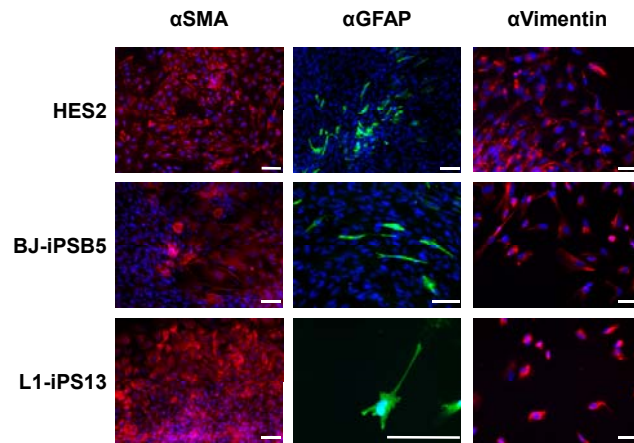


Supplementary Figure 7. Gene expression analysis. **a**, qPCR was used to evaluate the expression of *hGDF3*, *hDPPA4*, *hREX1* and *hTERT* in two LS-iPSC lines from each patient and compared to their parental fibroblasts. HES2 cells were used as positive control of pluripotency gene expression. PCR reactions were normalized against β -*ACTIN* and represented relative to the expression in HES2 cells. **b**, Two sample comparison plots of log₂ expression values with the line $Y=X$ as a basis for comparison along with $Y = X \pm 1$ or 2 lines, representing 2-fold and 4-fold expression changes, respectively. In each scatter-plot the position of *SOX2*, *LIN28* and *OCT4* transcription factors is indicated.

a

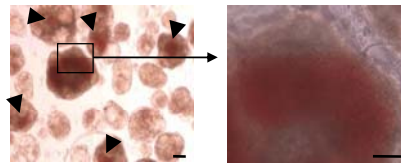


b

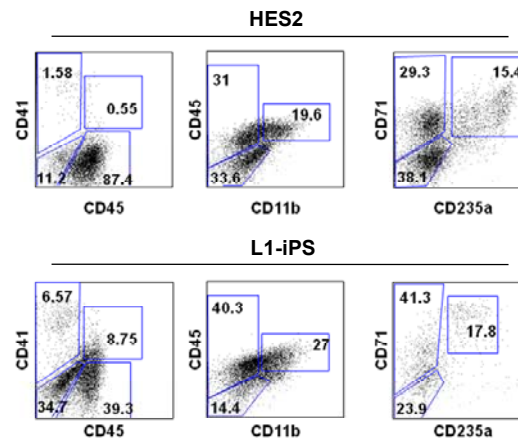


Supplementary Figure 8. *In vitro* differentiation of iPSC lines. a, Day 8 EBs of HES2, BJ-iPSB5, L1-iPS13 and L2-iPS6 cells. **b,** After 16 days of differentiation, cells were stained with SMA, GFAP and Vimentin antibodies. Scale bar, 100 μ m.

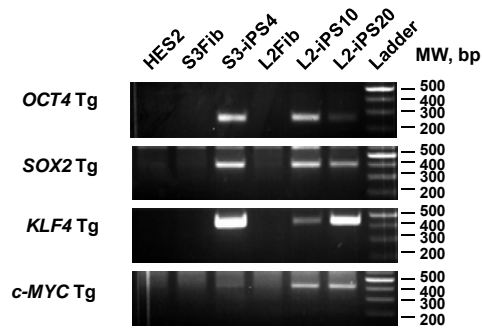
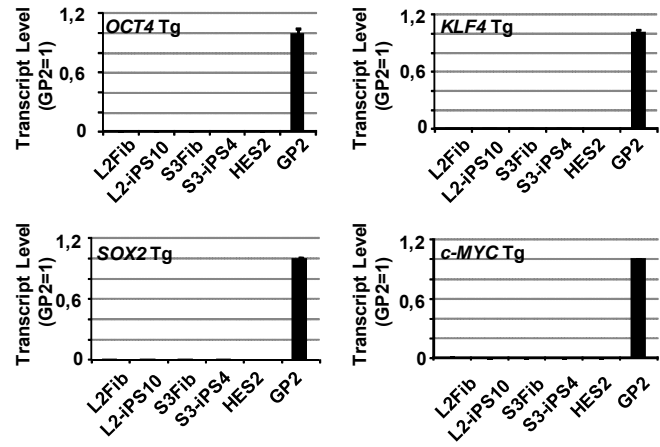
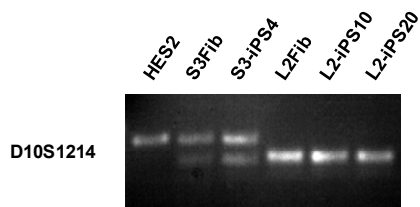
a



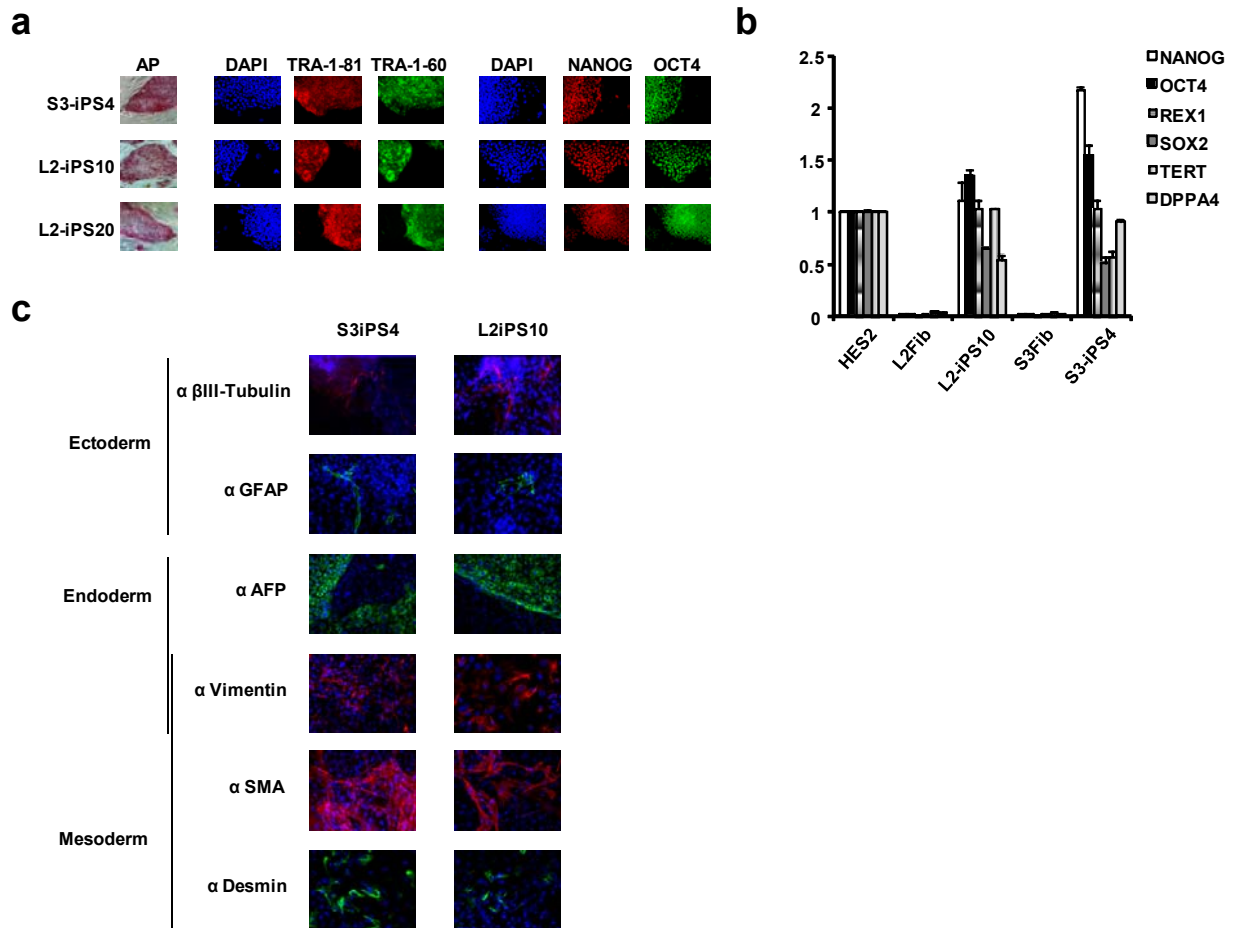
b



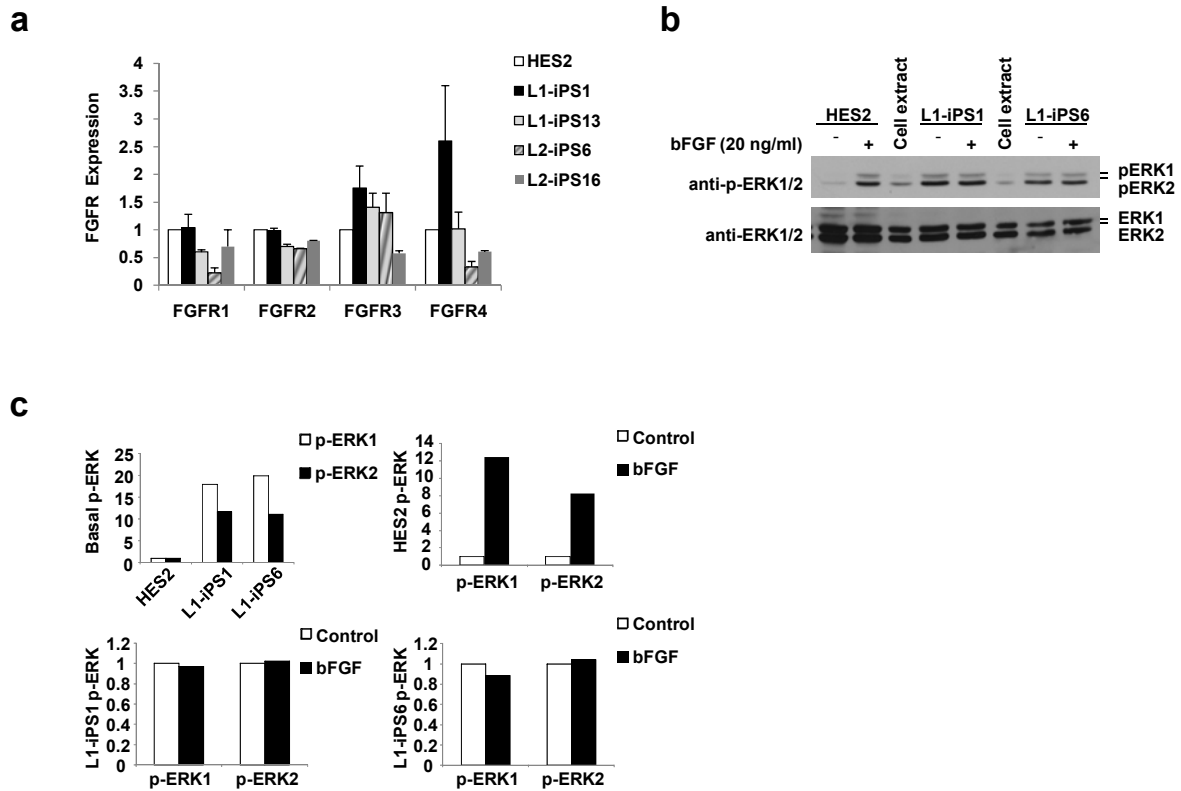
Supplementary Figure 9. LS-iPSC differentiate into hematopoietic cells. a, Red EBs, an indication of erythrocyte development, can be observed in L1-iPSC plates 14 days after differentiation. Scale bar, 100 μ m. **b,** CD41, CD45, CD11b, CD71 and CD235a hematopoietic markers were analyzed by flow cytometry in EBs derived from HES2 and L1-iPSC, 18 days after induction of hematopoietic differentiation.

a**b****c**

Supplementary Figure 10. Characterization of wt S3-iPS4 and L2-iPSC. **a**, The iPSC have the four transgenes integrated in their genome. **b**, Tg silencing analysis. **c**, Fingerprinting analysis of the iPSC lines using their parental fibroblasts and HES2 cells as controls.



Supplementary Figure 11. Pluripotency of S3-iPS4 and L2-iPSC. a-b, S3-iPS4, L2-iPS10 and L2-iPS20 expressed pluripotency markers. c, The iPSC differentiated into derivatives of the three germ layers.



Supplementary Figure 12. Disruption of MAPK activation upon bFGF stimulation in LS-iPSC. **a**, FGF receptors expression analysis by RT-qPCR in LS-iPSC and fibroblasts compared to HES2. **b**, L1-iPS1, L1-iPS6 and HES2 cells were serum- and bFGF-starved overnight. The following day, the cells were treated with bFGF for 10 minutes (+) or not (-). Total ERK1/2 and p-ERK1/2 expression was analyzed by immunoblotting of total lysates. **c**, Basal p-ERK1/2 was quantified in each sample and compared to HES2C (top left panel). The relative increase of p-ERK1/2 level upon stimulation was quantified in each sample (top right and lower panels). All the p-ERK1/2 values were normalized to their corresponding total ERK1/2 values.

Table 1. Primer sets for PCR reactions.

PCR for fingerprinting					Sequences (5' to 3')
D21S2055				F	ACAGAACCAATAGGCTATCTATC
				R	TACAGTAAATCACTTGGTAGGAGA
D10S1214				F	ATTGCCCAAAACTTTTTTG
				R	TTGAAGACCAGTCTGGGAAG
D17S1290				F	GCCAACAGAGCAAGACTGTC
				R	GGAAACAGTTAAATGGCCAA
qPCR for endogenous pluripotent genes					
GENE	Accession	Position	Size		Sequences (5' to 3')
hOCT4	NM_002701	1194-1217	123	F	AACCTGGAGTTTGTGCCAGGGTTT
		1293-1316		R	TGAACTTCACCTTCCCTCCAACCA
hNANOG	NM_024865	1120-1141	190	F	CCTGAAGACGTGTGAAGATGAG
		1288-1309		R	GCTGATTAGGCTCCAACCATAC
hDPPA4	NM_018189	1128-1148	223	F	AGTGCCTGTTGCTTTGTGAGT
		1330-1350		R	TGCACTGAACTGAGATTGCAC
hESRRB	NM_004452	1400-1423	181	F	GTACATCGAGGATCTAGAGGCTGT
		1557-1580		R	CAGTTTGACGCTATAGAAGTGCTG
hSOX2	NM_003106	108-132	150	F	AGAAGAGGAGAGAGAAAGAAAGGGAGAGA
		233-257		R	GAGAGAGGCCAAACTGGAATCAGGATCAAA
hREX1	NM_174900	1026-1047	267	F	AAAGCATCTCCTCATTTCATGGT
		1271-1292		R	TGGGCTTTTCAGGTTATTTGACT
hGDF3	NM_020634	829-850	231	F	CACCGTCACCAGCTATTCATTA
		1038-1059		R	GTAGAGCATGGAATGGGAGAC
hTERT	NM_198253	3198-3220	115	F	TGAAAGCCAAGAACGCAGGGATG
		3288-3312		R	TGTGAGTCAGCTTGAGCAGGAATG
h-β-ACTIN	NM_001101	1332-1353	169	F	TTTTTGCTTGACTCAGGATTT
		1479-1500		R	GCAAGGGACTTCCTGTAACAAC
qPCR for retroviral silencing			Size		Sequences (5' to 3')
qPCR-Tg- pMX				F	CCCTCAAAGTAGACGGCATC
qPCR-Tg-hOCT4			157	R	GCGAGAAGGCCAAAATCTGAA
qPCR -Tg-hSOX2			146	R	TTCAGCTCCGTCTCCATCAT
qPCR-Tg-hKLF4			168	R	GTGGAGAAAGATGGGAGCAG
qPCR-Tg-hc-MYC			291	R	AGGCTGCTGGTTTTCCAATA
PCR for retroviral integration			Size		Sequences (5' to 3')
PCR-Tg-pMX				R	GCTTGCCAAACCTACAGGTG
PCR-Tg-hOCT4			252	F	CCCCAGGGCCCCATTTTGGTACC
PCR -Tg-hSOX2			389	F	GGCACCCTGGCATGGCTCTTGGCTC
PCR-Tg-hKLF4			424	F	ACGATCGTGGCCCCGAAAAGGACC
PCR -Tg-hc-MYC			417	F	CAACAACCGAAAATGCACCAGCCCCAG
PCR for polymorphism detection			Size		Sequences (5' to 3')
			1194	F	TATGGCGTCATGCGTGTTAGG
				R	ACTGGCTTAATTCTCATTGGCC

F: Forward, R: Reverse